The Journal of Experimental Biology 208, 4627-4639
Published by The Company of Biologists 2005
doi:10.1242/jeb.01919

A test of mouth-opening and hyoid-depression mechanisms during prey capture in a catfish using high-speed cineradiography

Sam Van Wassenbergh[1,*], Anthony Herrel[1], Dominique Adriaens[2] and Peter Aerts[1]
[1]*Department of Biology, University of Antwerp, Universiteitsplein 1, B-2610, Antwerpen, Belgium* and
[2]*Evolutionary Morphology of Vertebrates, Ghent University, K. L. Ledeganckstraat 35, B-9000, Gent, Belgium*
*Author for correspondence (e-mail: Sam.VanWassenbergh@ua.ac.be)

Accepted 6 October 2005

Summary

Detailed morphological analyses have identified a number of different mechanical pathways by which the morphologically complex cranial system of fishes can achieve mouth opening and hyoid depression. However, many of these proposed mechanisms remain untested. Furthermore, very little is known about the precise timing of activity of each of these mechanisms, and about the magnitude of each mechanism's total contribution to its proposed function. In the present study, all mouth opening and hyoid depression mechanisms described for *Clarias gariepinus*, an air-breathing catfish, are analysed. High-speed X-ray videos were recorded during prey capture of three catfish implanted with small, radio-opaque markers in the cranial elements potentially involved. A kinematic analysis was performed from which data were used as input in planar four-bar models. This analysis shows that the opercular mouth-opening mechanism initiates mouth opening, but is not able to cause the complete mouth openings as observed on the X-ray videos. The latter is accomplished through the protractor hyoidei muscles, which couple hyoid depression to lower jaw depression in a four-bar system and also reinforce lower jaw depression by shortening during the final stage of mouth opening. Although the angulo-ceratohyal ligament was previously hypothesised to play a part in mouth opening, our results show that it probably does not, but rather functions as a hyoid-elevator during mouth closure. Finally, hyoid depression is exclusively achieved by the four-bar mechanism involving neurocranial elevation and pectoral girdle retraction, generally without any reinforcement by shortening of the sternohyoideus muscle. In contrast to the results from a recent analysis on sunfish, the catfish's sternohyoideus gradually elongates during hyoid depression.

Key words: X-ray video, kinematics, four-bar linkage, feeding, catfish, *Clarias gariepinus*.

Introduction

Fishes are known to have a morphologically complex and highly kinetic skull (Ferry-Graham and Lauder, 2001). The cranial musculo-skeletal system of adult teleost fishes consists of about 60 interconnected skeletal parts that are moved by an approximately equal number of muscles (Aerts, 1991). Since the early 20th century, functional morphologists have identified a large number of distinct, kinematic couplings between the elements of the head. They examined, for instance, couplings (or linkages) involved in protrusion of the jaws (Van Dobben, 1937; Alexander, 1970; Motta, 1984; Westneat and Wainwright, 1989; De La Hoz, 1994; De La Hoz et al., 1994; Waltzek and Wainwright; 2003; Ferry-Graham et al., 2001; Hulsey and Wainwright, 2003; Konow and Bellwood, 2005; Wainwright et al., 2005), depression of the lower jaw (Van Dobben, 1937; Otten, 1982; Aerts and Verraes, 1984; Westneat, 1990, 1994, 2004; Gibb, 2003; Durie and Turingan, 2004; Konow and Bellwood, 2005), depression of the hyoid (Elshoud-Oldenhave and Osse, 1976; Muller, 1987, 1996; Bergert and Wainwright, 1997) and abduction of the suspensorium (Elshoud-Oldenhave and Osse, 1976; Aerts, 1991; De Visser and Barel, 1996). Considerable insight into the behaviour of these systems has been achieved by modelling these as planar four-bar linkages, i.e. closed and intrinsically movable chains of four bars, of which one is immobile (Muller, 1996). In this way, understanding has been gained in the transmission of force and velocity between coupled elements of the fishes' head.

An additional aspect of the functional complexity of the cranial system in fishes is that some essential functions during feeding and respiration, such as opening the mouth or rotating the hyoid ventrally, can be achieved by more than one mechanism at the same time. According to morphological studies, the majority of adult teleosts are theoretically able to depress their lower jaw using four mechanisms (Diogo and Chardon, 2000), which are illustrated in Fig. 1 for *Clarias gariepinus*, the species studied here: (1) the opercular four-bar mechanism in which dorso-caudal rotation of the opercular bone (realised by contraction of the levator operculi muscle) retracts the interopercular bone and a ligament connecting this bone to the lower jaw (Fig. 1A), (2) a hyoid four-bar

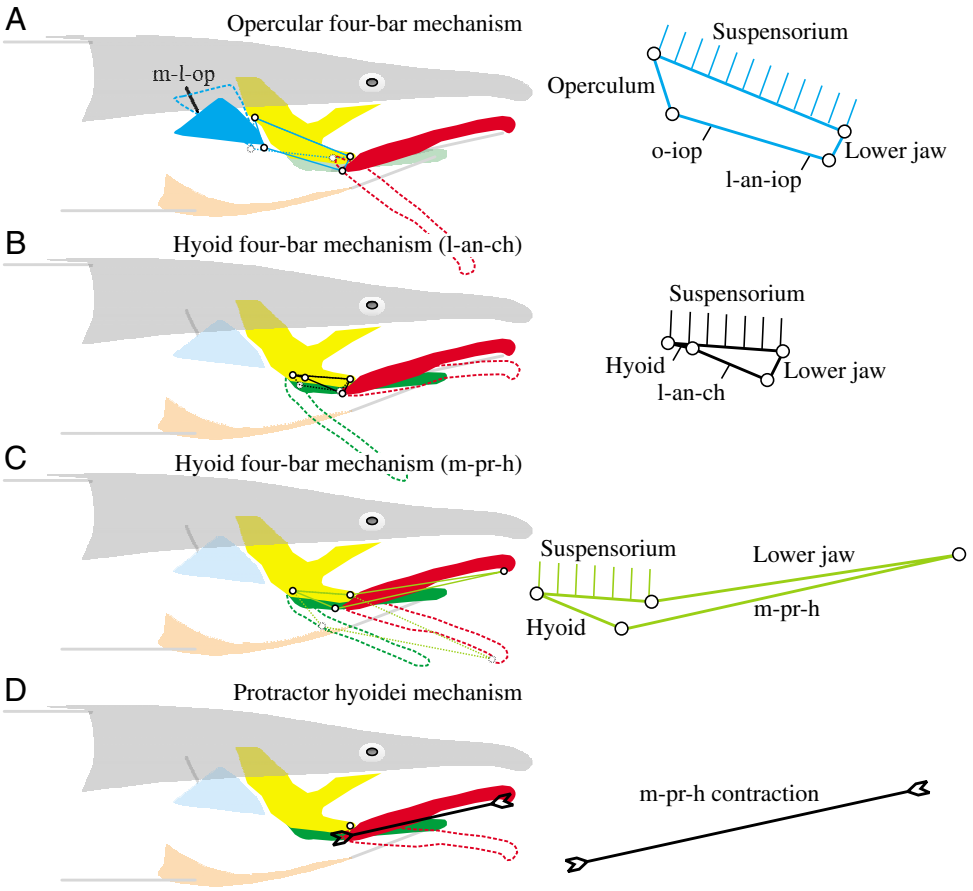

Fig. 1. Schematic representation of the four potential mouth-opening mechanisms (A–D) in *Clarias gariepinus*. The functional elements of the cranial system are represented by different colours: lower jaw, red; hyoid, green; suspensorium, yellow; operculum, blue; cleithrum, yellow and neurocranium, grey. Dark and light colours represent elements that are involved and not involved, respectively, in a particular mechanism. Broken lines correspond to positions of cranial elements and four-bar chains after activity of the mechanisms. More detailed representations of the four-bar systems are given on the right, in which the fixed link is represented by short perpendicular lines. l-an-ch, ligamentum angulo-cerotohyale; l-an-iop, ligamentum angulo-interoperculare; m-l-op, musculus levator operculi; m-pr-h, musculus protractor hyoidei; o-iop, os interoperculare.

mechanism in which lower jaw depression is generated by a ligament between the hyoid and the lower jaw (ligamentum angulo-ceratohyale) that is pulled ventro-caudally when the hyoid is depressed (Fig. 1B), (3) a second hyoid four-bar mechanism in which the coupling between the hyoid and the lower jaw is established by the protractor hyoidei muscles (Fig. 1C) and (4) contraction of the protractor hyoidei itself (Fig. 1D), which will reinforce the action of the previous mechanism in case of ongoing hyoid depression.

A similar situation occurs for the depression of the hyoid apparatus, which can be achieved by two mechanisms (Fig. 2): (1) a four-bar mechanism involving neurocranial elevation and pectoral girdle retraction (Fig. 2A; see also Muller, 1987; Bergert and Wainwright, 1997) and (2) contraction of the sternohyoideus muscle, which will reinforce the action of the first hyoid depression mechanism in case neurocranial elevation and/or pectoral girdle retraction is taking place (Fig. 2B). Both cases, however, require at least a fixation of the pectoral girdle by the hypaxial muscles.

Despite the large amount of literature on mechanisms of mouth opening and hyoid depression in fish, very little is known on how these different mechanical pathways operate *in vivo* when carrying out their proposed functions. Do all mechanisms contribute simultaneously during the entire mouth opening or hyoid depression? Or are there mechanisms that only perform their proposed function during the initial phase of lower jaw or hyoid motion, while others are active at later instants? Concerning the opercular mouth-opening mechanism, for example, it has been suggested that this mechanism has a role in initiating lower jaw depression in cichlids (Aerts et al., 1987; Durie and Turingan, 2004). For some other fish, however, kinematic studies have reported opercular rotations continuing until the mouth reaches its maximal gape (e.g. Elshoud-Oldenhave and Osse, 1976; Lauder, 1982; Konow and Bellwood, 2005), which could imply that the opercular mouth opening mechanism is active for longer than just during the initial stages of mouth opening. A theoretical modelling of ontogenetic shifts in efficiencies of both the opercular and hyoid four-bar linkage systems has focused on their complementary contributions to mouth opening (Adriaens et al., 2001). Yet, no study to date has actually demonstrated the precise timing by which the opercular mechanism contributes to mouth opening. The same is true for the other mechanisms (Figs 1, 2), which, furthermore, have been addressed in considerably fewer studies compared with the opercular mechanism (Westneat, 1990, 1994).

In the present study, mouth opening and hyoid depression mechanisms are analysed during prey capture in an African air-breathing catfish *Clarias gariepinus*. By using planar four-bar models with kinematic data input from high-speed X-ray video recordings, we test the activity of all potential mechanisms

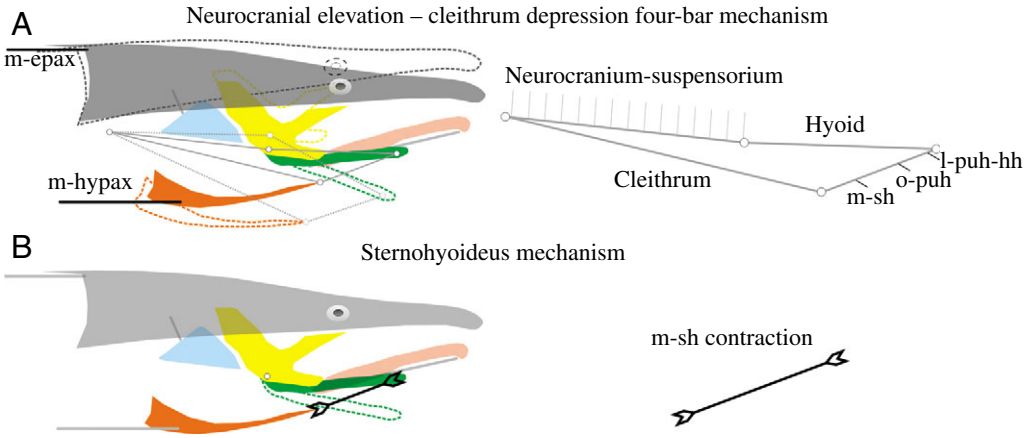

Fig. 2. Schematic representation of the two potential hyoid-depression mechanisms (A,B) in *Clarias gariepinus*. Colours and symbols correspond to those in Fig. 1. l-puh-hh, ligamentum parurohyalo-hypohyale; m-epax, epaxial muscles; m-hypax, hypaxial muscles; m-sh, musculus sternohyoideus; o-puh, os parurohyale.

described for both functions in this species (Adriaens et al., 2001). In particular, we will focus on the timing of the action and the relative contribution of each of the mouth-opening and hyoid-depression mechanisms.

Materials and methods

Study animals

Clarias gariepinus Burchell 1822 is an air-breathing catfish (Family Clariidae) with an almost Pan-African distribution that is also found in rivers and lakes of the Middle East and Turkey (Teugels, 1996). This species was chosen because multiple mechanisms of mouth opening and hyoid depression have been suggested previously based on morphological studies (Adriaens et al., 2001). As jaw protrusion is absent in Clariidae and other catfishes (Alexander, 1965), *C. gariepinus* also has the advantage over many other teleosts in that jaw protrusion mechanisms do not interfere with lower jaw depression mechanisms, which will simplify the analysis.

Three adult catfish were used in the experiments, with cranial lengths of 70.2, 94.1 and 74.5 mm (defined as the distance between the rostal tip of the premaxilla and the caudal tip of the occipital process). These individuals will be referred to as, respectively, catfish A, B and C. These catfish were aquarium-raised specimens obtained from the Laboratory for Ecology and Aquaculture (Catholic University of Leuven, Belgium). The animals were kept in separate 20 l test aquaria and were trained to capture food inside a narrow, projecting corridor (25 cm length, 8 cm width, 15 cm water height) of the aquarium. The thin Plexiglas walls (2 mm) of the corridor minimised the amount of X-ray absorption.

Radio-opaque marking

In order to increase the quantification accuracy of movements of cranial bones (see further), small metal markers were inserted subcutaneously, touching the bones at specific positions of interest, using hypodermic needles. Prior to implantation of these radio-opaque markers, the animals were anaesthetised with MS222 (Sigma Chemical Company, St Louis, MO, USA). In this way, 13 markers were inserted and used to track the movements of the lower jaw, hyoid, operculum, cleithum and neurocranium in each individual (Fig. 3). Occasionally, a single marker was expelled from the skull between the marking period and the recording sessions. This was the case for the rostral tip of the cleithrum in two individuals (cranial lengths of 74.5 and 94.1 mm). These individuals also have two markers on the operculum instead of one opercular and one suspensorial marker, as shown for the individual in Fig. 3.

Radio-opaque markers were implanted left and right at the basis of the lower jaw, hyoid and cleithrum (Fig. 3), as this procedure allows a more accurate measurement of kinematics in the case of minor rotations of the fish along its medio-sagittal axis during the feeding event (Van den Berg, 1994). Note, however, that prey capture sequences were discarded in cases where our catfish showed substantial rotation along axes other than parallel to the camera lens, or if initially the mid-sagittal plane of the fish diverged significantly from perpendicular to the camera lens axis.

After the recording sessions, the animals were killed by an overdose of MS222. Next, additional markers were inserted (single side only) onto some critical points in the four-bar mechanisms for mouth opening and hyoid depression. These points are the articulations between suspensorium–operculum, operculum–interoperculum, interoperculomandibular ligament and anguloceratohyal ligament–retroarticular process of mandible, mandibulum–quadratum, suspensorium–hyoid and hyoid–anguloceratohyal ligament. During this post-recording marking, the precise positions of the four-bar joints for each individual were determined by careful observation, manipulations of structures and some dissections (e.g. removing the branchiostegal membrane to pinpoint the hyoid linkages).

X-ray video recording and digitisation

High-speed X-ray videos and photographs were recorded using a Philips Optimus X-ray generator (Royal Philips Electronics NV, Eindhoven, The Netherlands) coupled to a 14-inch image intensifier with two zoom modes (10 and 6 inch)

and a Redlake (SanDiego, CA, USA) Motion Pro camera (1248×1024 pixels). Videos were made in lateral view and were recorded at 250 frames per second, using the 6-inch zoom function (Fig. 4). Three prey types were used: (1) pieces of cod fillet and (2) unpeeled North Sea shrimps attached to a plastic-coated steel wire, and (3) small, spherical pieces of shrimp meat loosely attached to the tip of a needle. For each individual, 20 recordings were analysed (5, 5 and 10 sequences for each prey type, respectively).

The sixteen anatomical landmarks shown in Fig. 3 were digitised frame-by-frame from the high-speed X-ray videos using Didge (version 2.2.0, Alistair Cullum, Creighton University, Omaha, USA). The coordinates of all landmarks were recalculated to a frame of reference moving with the neurocranium. In this frame, the upper jaw tip was taken as origin and the horizontal axis is parallel to the roof of the buccal cavity (see Fig. 3). This digitisation and recalculation of reference frame was also done on the X-ray photographs with the additional markers on the four-bar joints (see above) together with the original, pre-recording markers. As the cleitrum can be distinguished reasonably well on the X-ray videos (Fig. 4) the tip of the cleithrum could still be digitised accurately in case the marker at this location was absent.

Angles in the first (upper right) and fourth (lower left) quadrant of the reference frame (Fig. 3) are, respectively, negative and positive. Consequently, kinematic profiles of mouth opening (mechanically identical to lower jaw depression in Clariidae) and hyoid depression will give rising curves. On the other hand, mouth closing and hyoid elevation will be represented by descending curves.

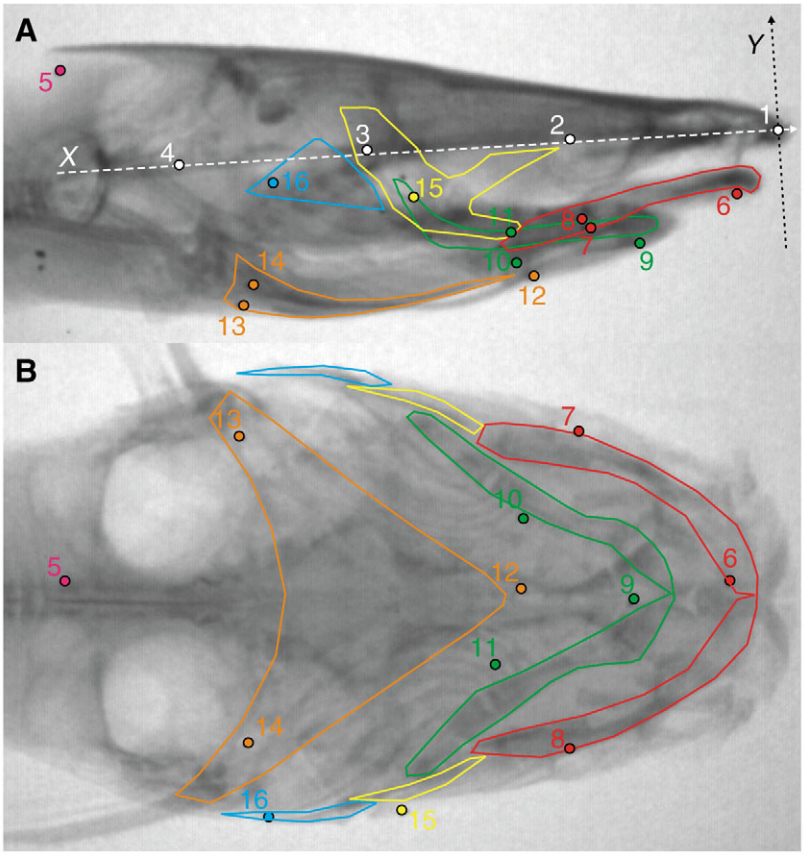

Fig. 3. Position of the inserted radio-opaque markers (coloured circles) and additional landmarks (white circles) digitized to define the fish-bound frame of reference (white broken lines) imposed on a lateral (A) and dorsoventral (B) X-ray image of *Clarias gariepinus* (70.2 mm cranial length). Contours of the lower jaw (red), hyoid bars (green), cleithrum (orange), suspensorium (yellow) and operculum (blue) are shown. The markers are: (1) the upper jaw tip, (2–4) landmarks on the roof of the buccal cavity, (5) anterior of the neurocranium, close to the occipital process, (6) lower jaw tip, (7,8) more caudal points on the left and right lower jaw, (9) rostral tip of the hyoid, (10,11) approximate middle along left and right hyoids, near the origin of the protractor hyoidei muscles, (12) tip of the cleithrum, (13,14) caudal points on the left and right side of the cleithrum, near the base of the pectoral fins, (15) suspensorium and (16) operculum. Landmark (1) was taken as origin (0,0) and the *X*-axis is parallel to the least-squares linear regression through points (1–4).

Muscle lengths

The origin-to-insertion length (in the sagittal plane) of the sternohyoideus muscle (mechanism Fig. 2B) was calculated as the distance between the tips of the cleithrum and the hyoid (landmarks 12 and 9 of Fig. 3). Note that a part of the short parurohyale bone is included into this 'sternohyoideus length'. The length of the protractor hyoidei muscles (mechanism Fig. 1D) was directly calculated from the *XY*-coordinates of the landmarks near its origin and insertion (landmarks 10,11 and 6 of Fig. 3). These muscle origin-to-insertion lengths will be presented as a percentage of the average muscle length observed for each individual. If muscle-shortening velocities are higher than 5% s^{-1} after 5 Hz Butterworth filtering (see below), shortening velocities exceed the observed level of noise for these measurements. In that case only, muscle shortening is assumed to be significant.

Four-bar models

The terminology of four-bar systems used in this paper will adhere to the one used in mechanical engineering. Consequently, the fixed bar is called the 'frame'. The two bars connected to the frame are named 'follower' and 'crank'. The crank is the input link, i.e. the link on which the input force is acting. The crank and the follower are connected to the ends of the 'coupler'. As a given four-bar chain has only one degree of freedom, its entire configuration depends on the angle between crank and frame (referred to as 'input angle'). In this way, the angle between follower and frame (referred to as 'output angle') was calculated in function of the input angle according to Aerts and Verraes (1984). As most often there existed two solutions for output angle (see Aerts and Verraes, 1984), a

graphical check was performed (intersecting circles using CorelDraw) to determine the anatomically correct solution. To refer to one of the mouth-opening or hyoid-depression mechanisms, we will use its number as presented in Fig. 1 or Fig. 2 from this point on.

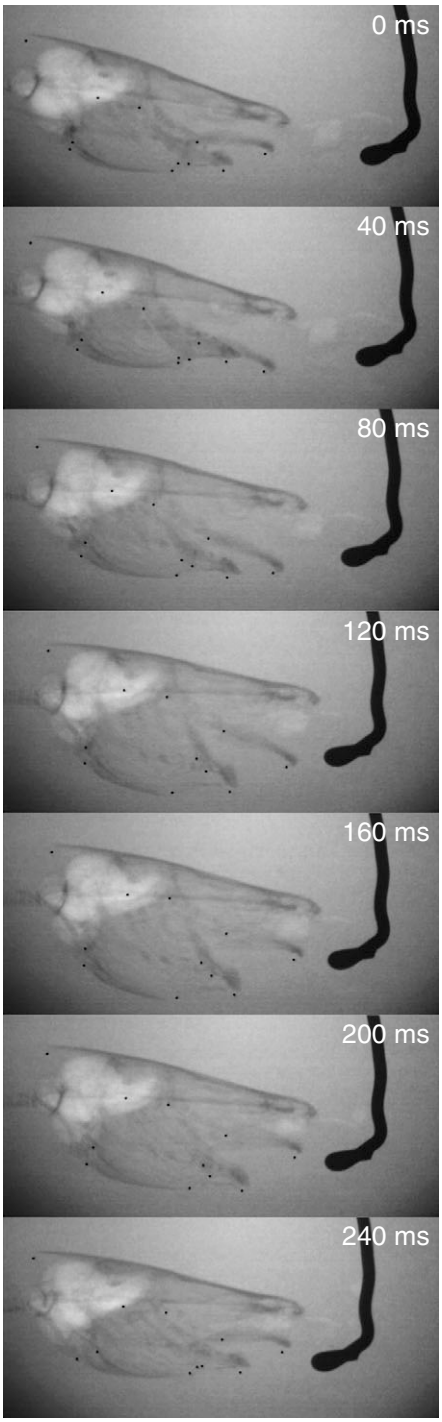

Fig. 4. Selected X-ray video frames from a representative prey capture sequence (0–240 ms) of a *Clarias gariepinus* individual (70.2 mm cranial length, Catfish A) equipped with radio-opaque markers during feeding on an attached shrimp.

In order to calculate rotations of the lower jaw or hyoid caused by the action of a four-bar system and to compare this data to the observed lower jaw and hyoid rotations, four types of data were collected with respect to each four-bar mechanism: (1) the coordinates of the four corners (point-joints) of the four-bar system, (2) the fixed angle between the four-bar's crank and the line connecting the two radio-opaque markers on the bone serving as crank, which is necessary to translate measured positions of these markers with respect to the cranium to instantaneous positions of the crank in the four-bar system, (3) the rotation of this segment (i.e. the line connecting the markers on the crank) over time and (4) the fixed angle between the four-bar's follower and the line interconnecting the two markers on the lower jaw (for mouth opening four-bars) or on the hyoid (for hyoid depression four-bars). With these data, the initial four-bar configuration, changes in the input and output angles of the four-bar system, and the corresponding positions of the lower jaw or hyoid with respect to the fixed, fish-bound frame (Fig. 3) due to action of the four-bar system were calculated.

For mechanism 1A (Fig. 1A), the *XY*-coordinates of all four-bar corners were obtained from the post-recording marking (see above). For the individual lacking one of the two radio-opaque markers on the operculum (Fig. 3), the fixed coordinate of the operculum–suspensorium joint was used instead. For mechanism 1B (Fig. 1B), the position of hyoid-attachment of the angulo–ceratohyal ligament with respect to the hyoid was determined based on the morphological data (Adriaens et al., 2001). To calculate the angle of the lower jaw, hyoid and cleithrum with respect to the *X*-axis, the line interconnecting the tip landmark (respectively landmarks 6, 9 and 12 of Fig. 3) and the average between the coordinates of the left and right caudal landmarks on these structures (respectively landmarks 7, 8, 10, 11, 13 and 14 of Fig. 3) were used.

For mechanism 2A (Fig. 2A) and mechanism 1C (Fig. 1C), the position of the centre of rotation of the cleithrum and the hyoid, and the length of the crank, were calculated for each video sequence separately. This was done by using the kinematic data from the markers inserted at two positions (tip and caudal) on the cleithrum or hyoid.

In these four-bar linkage models, the suspensoria are assumed to be immobile with respect to the neurocranium. Although *Clarias gariepinus* shows some abduction (lateral swing) of the suspensoria during the expansive phase of suction feeding, the total lateral expansion is only a small fraction of the observed ventral expansion of the cranial system in this species (Van Wassenbergh et al., 2004). Furthermore, as the suspensoria are relatively short in this dorsoventrally flattened fish (Fig. 1), abduction of the suspensoria will only have a small influence on the relative position of the four-bar point-joints in a lateral view. As a consequence, this assumption seems justified and will probably not influence the results significantly.

Because of the short distance between the landmarks determining opercular rotation, digitisation noise had to be reduced by filtering. Therefore, a fourth order, zero phase-shift

Butterworth filter was used according to Winter (2004), with cut-off frequencies between 10 and 20 Hz, depending on the nature of the data-noise. This filtering procedure was also performed prior to differentiation (e.g. calculating velocities), and where the tip of the cleithrum had to be digitised without marker (see above). Thus, with the exception of lower jaw movements predicted by the opercular mechanism (Fig. 1A) and the hyoid movements predicted by mechanism 2A (Fig. 2A) in two out of the three individuals, all data presented as angle *vs* time are (or directly use) unfiltered kinematic data.

The coupler of two of the four-bar systems (Figs 1C, 2A) consists of a muscle. In contrast to ligaments or bones, muscle cannot be considered as a link of constant length (as assumed in four-bar models). Therefore, in addition to calculating four-bar model output with the starting length of the muscle (at time 0), the four-bar simulations were performed using the minimal and maximal lengths for that muscle during a given prey capture sequence. To do so, the length of the coupler was lengthened or shortened without changing the input angle of the four-bar system. Consequently, only the output angle and the predicted lower jaw or hyoid angle will change by adjusting the coupler's length in this way.

Data interpretation and statistics

As mentioned earlier, the result of the action of a certain four-bar model will be presented as a predicted lower jaw or hyoid angle. This model output can be directly compared to the observed lower jaw or hyoid kinematics. However, for mechanisms 1A and 1B, the length of the coupler is constant (Fig. 1A,B), while this is not required in mechanism 1C and 2A (Figs 1C, 2A). Thus, the data interpretation depends on the type of the four-bar system considered (i.e. with or without constant length coupler).

If the coupler can be assumed to have a constant length, then the four-bar system will contribute to mouth opening if the predicted lower jaw angle coincides with the observed lower jaw angle. If not, from a morphological point of view this means that the coupler's ligament (l. angulo–interoperculare in mechanism 1A or l. angulo–cerotohyale in mechanism 1B) is not tight and little or no force will be transmitted by this mechanism. 'Coinciding' and 'not coinciding' are distinguished by performing one-way analyses of variance (ANOVA) with a repeated-measures design, with the observed and predicted lower jaw/hyoid angle as independent variables. By adjusting the amount of data points included in the analyses, the time at which both curves become significantly distinct ($P<0.05$) is determined. These statistics were performed using SPSS v. 12.0 (SPSS Inc., Chicago, IL, USA).

If the coupler is a muscle and thus has a variable length, data interpretation is more complex. Four-bar simulations with muscle at its starting length show how the lower jaw or hyoid would behave in the case that the muscle keeps its initial length throughout the entire prey capture sequence. Four-bar simulations with muscle at its maximal length show the minimal mouth opening or minimal hyoid depression that is exclusively the result of the four-bar action, without any reinforcement by muscle shortening. Because we cannot exclude the possibility that m. protractor hyoidei or m. sternohyoideus lengthen during expansion *a priori*, four-bar simulations with muscle at its minimal length were also added (see above). These four-bar simulations show the mouth opening or hyoid depression in the case of full and constant reinforcement by muscle shortening throughout the entire sequence. In other words, the simulations at maximal and minimal length muscle reveal the boundaries of the four-bar mechanism, while muscle shortening (Figs 1D, 2B) cause the fluctuation between these boundaries. For example, if the m. sternohyoideus shortens gradually and reaches its minimal length at the instant of maximal hyoid depression, the predicted hyoid angle from the four-bar model with the muscle at starting length shows how many degrees of hyoid rotation are due to mechanism 2A at that instant, while the difference between the hyoid angle actually observed and this four-bar prediction is due to sternohyoideus shortening.

For mechanism 1D (Fig. 1D), we cannot discern *active* muscle shortening from *passive* muscle shortening whenever mechanisms 1A or 1B are also contributing to mouth opening. However, if muscle shortening is the only explanation for the observed lower jaw or hyoid movement, it can be safely considered as an *active* muscle shortening. Note in this respect that despite several attempts by the author, EMG measurements during prey capture in *C. gariepinus* were not successful due to the erratic behaviour of this species.

Most results will be presented as mean kinematic profiles per individual. In order to account for strike-to-strike variability and to avoid the potential confounding effects on kinematic means, the time axis of each prey capture sequence was scaled to the total duration of mouth opening (or hyoid depression) of that sequence. Consequently, timings of mouth opening and hyoid depression mechanisms are expressed as a percentage of mouth opening duration, with 0% being the start of mouth opening and 100% the time of maximal gape. Linear interpolations are used to extract data at 2% intervals on this new, relative time scale. Another advantage of this procedure is that effects of differences in body size on the speed of prey capture kinematics (see Van Wassenbergh et al., 2005) are removed, thus simplifying the comparison between individuals.

When comparing the characteristics of different types of mouth opening (see below), two-way, mixed model ANOVAs were used. In these statistics, the effects of mouth opening type (fixed factor) are tested, with individual as a random factor. A sequential Bonferroni correction was applied (to adjust the significance level according to the number of tests that were carried out) in case of consecutive univariate testing.

Results

Mouth opening types

Based on the shape of the kinematic profiles of mouth opening during prey capture in *C. gariepinus*, two types of mouth opening could be distinguished (Fig. 5). In most of the

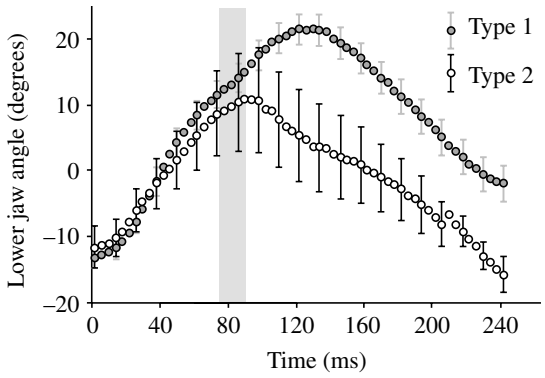

Fig. 5. Kinematic profiles of the two mouth-opening types observed in *C. gariepinus*, as illustrated for one individual (catfish A). Values are means ± S.E.M. (*N*=15 for Type 1; *N*=5 for Type 2). The grey bar indicates the period of the additional acceleration that can be observed during 'type 1' mouth opening. See text for further information.

prey capture sequences analysed (67%), an additional deceleration–acceleration can be discerned during mouth opening. In the other cases (33% of total), the shape of the mouth opening profile roughly approximates the ascending part of a sinusoidal function, with only a single acceleration and deceleration phase (Fig. 5). When occurring, the additional acceleration starts on average at 64.4±9.3% (mean ± S.D.) and ends at 84.0±4.8% of mouth opening. As distinct mouth-opening profiles can be caused by differences in the action of the mouth-opening mechanisms, these two types of mouth opening will be treated separately. The dominant mouth-opening type (which includes an additional deceleration–acceleration) will be referred to as 'type 1', while the less frequently occurring type (single deceleration–acceleration) is designated 'type 2'.

While both mouth-opening types could be discerned for each individual, the distinction between both types was most prominent in catfish A (Fig. 5). In this individual, these mouth-opening types also differed in maximal lower jaw depression angle. The additional acceleration of the 'type 1' mouth openings occurred approximately at the time the 'type 2' mouth openings reach maximal gape (Fig. 5). In catfishes B and C, however, no differences between the average kinematic profiles of 'type 1' and 'type 2' could be discerned (*P*=0.12 for B and *P*=0.67 for C).

Mechanism 1A

Mechanism 1A (Fig. 1A) is limited to the initial phase of mouth opening, as illustrated by the match between the observed lower jaw angle and the lower jaw angle predicted by the movement of this four-bar system during that time (Figs 6, 7). The time after the start of mouth opening to the moment at which this mechanism finishes its contribution to mouth opening varies among individuals, reflecting the inter-individual variation in opercular rotation. On average, this mechanism is active during the first 30%, 14% and 74% of the 'type 1'mouth opening phase (Fig. 6) for, respectively, catfish

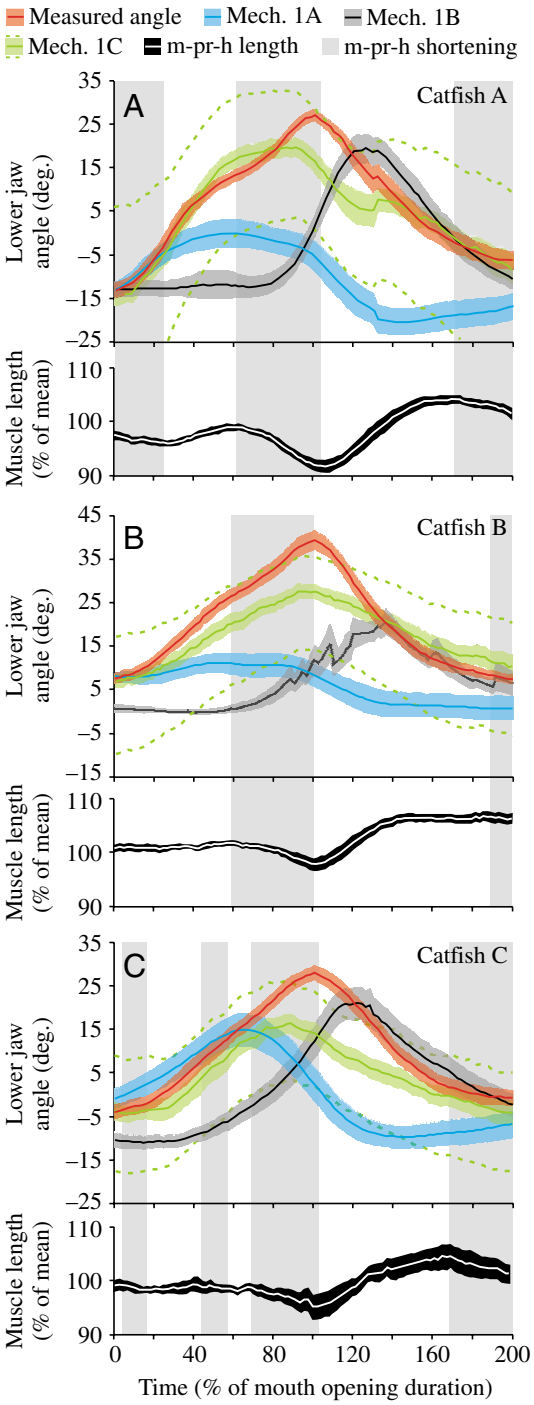

Fig. 6. Mean mouth-opening (0–100%) and mouth-closing (100–200%) profiles with the calculated four-bar model output for each of the mouth opening mechanisms during 'type 1' mouth openings (A–C, top), together with length of the protractor hyoidei (m-pr-h; A–C, bottom). Separate graphs are shown for each individual: A (*N*=15), B (*N*=12) and C (*N*=13). Grey bars indicate the time during which the protractor hyoidei shorten. The shaded areas accompanying each curve indicate S.E.M. The broken, green curves give average four-bar model output of mechanism 1C with the protractor hyoidei at minimum length (upper curve) and at maximum length (lower curve) as coupler. Colour codes are indicated in the key above the figure. Mech. 1A,1B,1C, see Fig. 1.

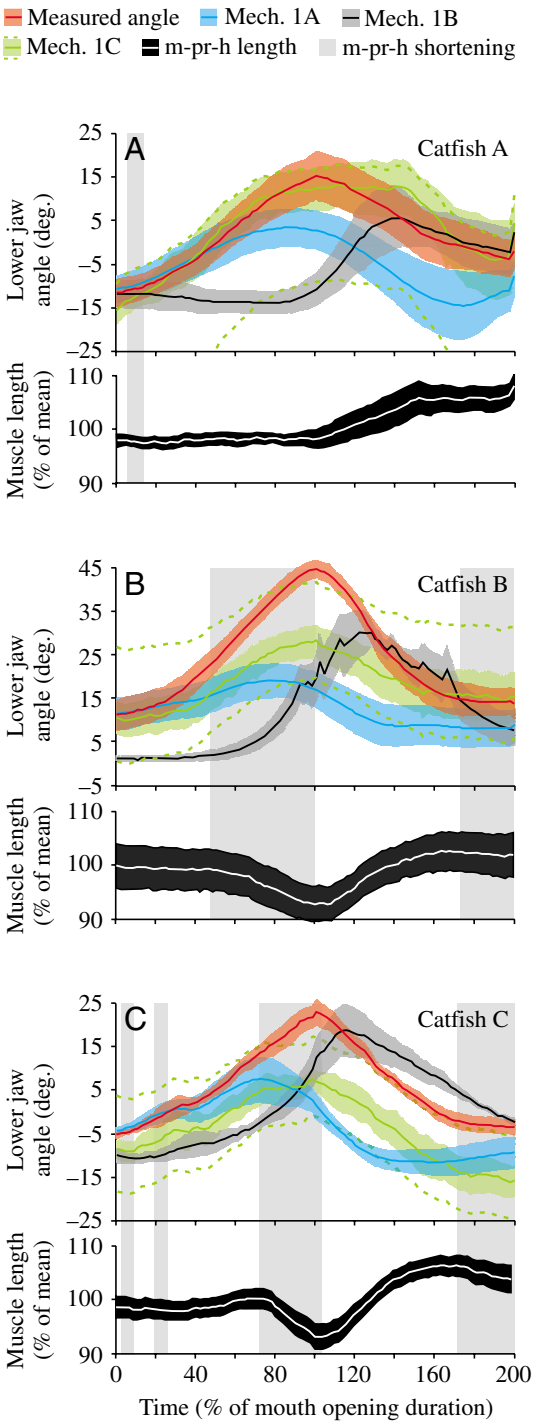

Fig. 7. Mean mouth opening (0–100%) and closing (100–200%) profiles with the calculated four-bar model output for each of the mouth opening mechanism during 'type 2' mouth openings (A–C, top), together with length of the protractor hyoidei (m-pr-h; A–C, bottom). Separate graphs are shown for each individual: A (*N*=5), B (*N*=8) and C (*N*=7). Grey bars indicate the time during which the protractor hyoidei shorten. The shaded areas accompanying each curve indicate S.E.M. The broken, green curves give average four-bar model output of mechanism 1C with the protractor hyoidei at minimum length (upper curve) and at maximum length (lower curve) as coupler. Colour codes are indicated in the key above the figure. Mech. 1A,1B,1C, see Fig. 1.

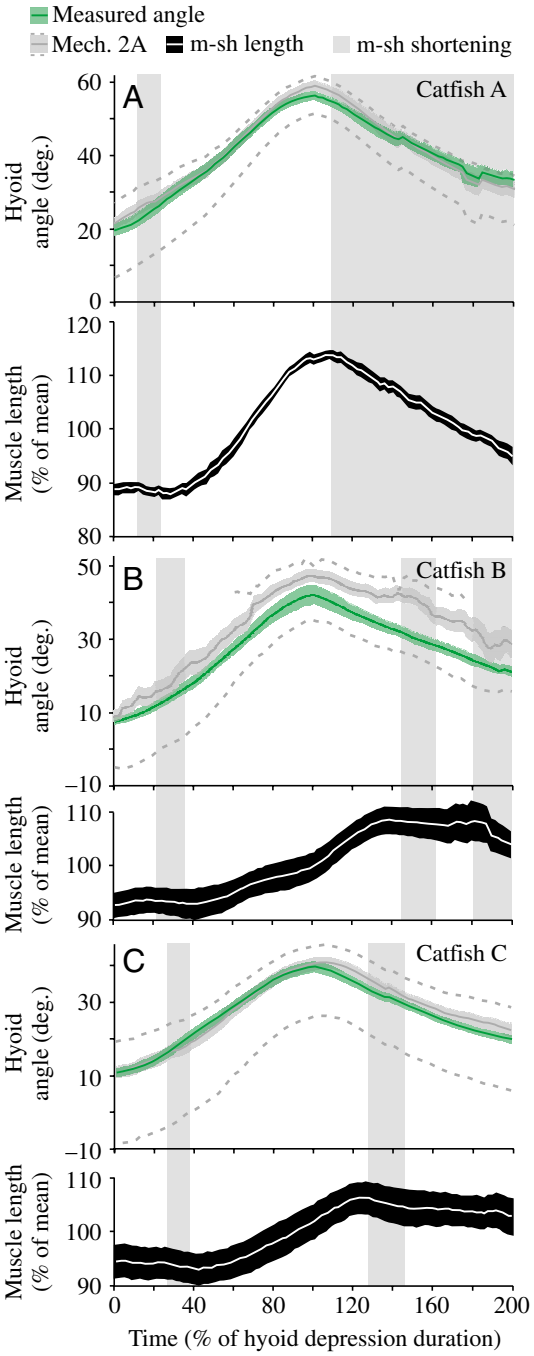

Fig. 8. Mean hyoid depression (0%–100%) and elevation (100%–200%) profiles with the calculated four-bar model output for hyoid-depression mechanism 2A (A–C, top), together with length of the sternohyoideus muscle (m-sh; A–C, bottom). Separate graphs are shown for each individual (*N*=20). The shaded areas accompanying each curve indicate S.E.M. Note that these S.E.M. values are larger in case the radio-opaque marker is absent at the tip of the cleithrum (B,C). The lower and upper broken, grey lines represent the output of the four-bar model with, respectively, a fully elongated sternohyoideus muscle and the sternohyoideus at minimum length. The latter curve is partly not displayed in B when there were no analytical four-bar solutions in more than half of the cases. Grey bars indicate the period during which the sternohyoideus shortens. Colour codes are indicated in the key above the figure. Mech. 2A, see Fig. 2.

A, B and C. This relative duration of mechanism 1A tends to be longer during the 'type 2' mouth openings, with 96%, 30% and 76% respectively, but this is not statistically different from the results for 'type 1' (ANOVA, $F_{1,2}$=2.08, P=0.29).

Mechanism 1B

Mouth opening mechanism 1B (Fig. 1B) is not active during any time of the mouth opening phase (Figs 6, 7). The only instants at which the lower jaw angle predicted by the activity of this four-bar mechanism coincides with the observed lower jaw angle during mouth opening, are near the start of jaw opening, when mechanism 1B -output does not cause any lower jaw rotation. Apart from these instants, lower jaw angles are consistently underpredicted (i.e. more elevated towards the neurocranium) by this mechanism during mouth opening (Figs 6, 7).

During mouth closing, however, the lower jaw profile predicted by mechanism 1B (Fig. 1B) generally converges towards, and finally becomes adjacent to the observed lower jaw angle (Figs 6, 7). Consequently, four-bar modelling predicts that only during mouth closing, the angulo–ceratohyal ligament becomes fully stretched and potentially couples hyoid to lower jaw movement. This situation, in which the observed and predicted lower jaw angles can no longer be distinguished statistically, takes place after 114%, 124% and 110% of mouth opening duration for the 'type 1' mouth openings, and after 118%, 124% and 108% for 'type 2' mouth openings in, respectively, catfish A, B and C.

Mechanism 1C

Without shortening of the protractor hyoidei muscles, mechanism 1C (Fig. 1C) alone would already be responsible for a large amount of lower jaw depression during hypaxial retraction of the pectoral girdle (Figs 6, 7). The average lower jaw rotations due to this mechanism are 32.7°, 20.6° and 20.1° ('type 1' mouth opening) for catfish A, B and C, respectively (Fig. 6), corresponding to 81.7%, 63.5% and 64.1% of the total observed lower jaw depression. The predicted maximal lower jaw angle by this four-bar mechanism is reached close to the time of maximal mouth opening (100%), more specifically at 86%, 96% and 88% for the three individuals studied. For the mouth-opening profiles of 'type 2', the absolute amount of lower jaw rotation that would be generated by this mechanism alone tends to be lower (ANOVA, $F_{1,2}$=21.6, P=0.043), with 25.0°, 17.1° and 13.1° for catfish A, B and C respectively (Fig. 7). However, the relative contribution to the total lower jaw depression is not (ANOVA, $F_{1,2}$=0.48, P=0.56). Again, maximal values of the lower jaw angles predicted by this mechanism are reached near the time of maximal gape (112%, 100% and 98%; Fig. 7).

Mechanism 1D

Mechanism 1D (Fig. 1D), shortening of the protractor hyoidei muscles (m-pr-h), will reinforce lower jaw depression caused by mechanism 1C. Relatively slow and brief m-pr-h shortening could sometimes be discerned during the first instants of mouth opening (Figs 6, 7). However, the relative contribution of this initial muscle shortening is limited, as mechanism 1C (four-bar system modelled without muscle shortening) still predicts the observed lower jaw accurately during this stage. Furthermore, in one of the three individuals studied (catfish B) no significant changes in the length of the m-pr-h were measured during the first half of the mouth opening phase (Figs 6B, 7B). As mechanism 1A also is active during this period, these muscle shortenings can either be passive or active.

A more extensive and faster shortening of the m-pr-h was observed during the final half of mouth opening. More specifically, this muscle starts shortening at 62%, 60% and 68% until, respectively, 104%, 102% and 104% of mouth opening ('type 1') in catfishes A, B and C (Fig. 6). In contrast to the limited m-pr-h shortenings during the first half of mouth opening, mechanism 1D now contributes significantly to mouth opening. As mechanisms 1A and 1B are not active during this period, and the predicted lower jaw profile by the action of mechanism 1C starts diverging from the observed lower jaw angle, active m-pr-h shortening must be responsible for depression of the lower jaw in surplus to the mechanism 1C-output (Figs 6, 7). This 'surplus' is on average 7.3°, 11.9° and 11.3° at the time of maximal mouth opening ('type 1') in our three catfishes.

For mouth openings of 'type 2', the results for catfish B and C (Fig. 7B,C) are similar to those during 'type 1' mouth opening, with respectively, m-pr-h shortening from 48% to 100% (16.6° surplus to mechanism 1C) and from 72 to 104% (14.9° surplus to mechanism 1C). However, for catfish A, the individual with the most diverging 'type 1' and 'type 2' profiles (see Fig. 5), no m-pr-h shortening could be discerned, not even during the last half of mouth opening (Fig. 7A). Consequently, only mechanism 1C causes lower jaw depression after the opercular mechanism (Fig. 1A) has ended its contribution during these sequences, without reinforcement by m-pr-h shortening.

Mechanism 2A

The four-bar system 2A (Fig. 2A) alone (i.e. without sternohyoideus shortening) is able to cause the entire hyoid rotation observed in *Clarias gariepinus* (Fig. 8). More specifically, 107.3%, 114.7% and 103.2% of the total hyoid depression is predicted by this mechanism if the sternohyoideus muscle maintains its initial (prior to expansion) length for, respectively, individuals A, B and C (Fig. 8). For individuals A and B, this corresponds to total hyoid rotations that are significantly higher than the observed hyoid rotations (P<0.001 and P=0.003). For individual C (Fig. 8C), the four-bar model output of mechanism 2A is not significantly different for the observed values from the start of hyoid depression until maximal hyoid depression (P=0.92).

The four-bar simulation with the sternohyoideus at maximal length predicted maximal hyoid angles of 51.4°, 32.6° and 26.3°, which corresponds to 86.6%, 79.4% and 53.7% of the total observed hyoid rotation in, respectively, catfish A, B and

C. If the sternohyoideus reached its minimal length (measured during the entire expansion–compression cycle) at the moment of maximal retraction of the cleithrum, then the four-bar system calculates hyoid angles of 61.5°, 50.9° and 45.4°. This corresponds to 114.2%, 125.1% and 119.5% of the observed maximal hyoid angle, or a surplus of 5.2°, 10.4° and 5.7° in hyoid rotation.

Mechanism 2B

Mechanism 2B (Fig. 2B), shortening of the sternohyoideus muscle (m-sh), will reinforce the hyoid depression caused by mechanism 2A. However, shortening of the m-sh during hyoid depression is limited in magnitude and restricted to a short period (Fig. 8). This period lasts (on average) from 12% until 24% (catfish A), 22% until 36% (catfish B) and 26% until 38% (catfish C) of the total hyoid depression duration. During these periods of m-sh shortening, the m-sh only shortens approximately 1% of its mean length. After this period, the muscle starts elongating (Fig. 8; see also Fig. 4). This elongation lasts approximately until maximal hyoid depression is reached (Fig. 8A,C), or even continues after peak hyoid depression in one individual (Fig. 8B). For all individuals, the m-sh is generally longer at the moment of peak hyoid depression than it is at the start of hyoid depression (Fig. 8).

Discussion

Mouth-opening mechanisms

The results of the present study show that during the first instants of mouth opening, opercular rotation causes lower jaw depression (through mechanism 1A; Fig. 1A). However, as some shortening of the protractor hyoidei muscles (mechanism 1D; Fig. 1D) also occurs during this time (Figs 6, 7), this does not necessarily imply that the opercular mouth-opening mechanism is the only mechanism used by *Clarias gariepinus* for initiating mouth opening. Unfortunately, we cannot distinguish whether these short bursts of protractor hyoidei shortening near the start of mouth opening are caused by muscle activity, or if they are merely the consequence of the rotating lower jaw caused by the opercular mechanism. Thus, initial mouth opening is performed by the opercular mechanism (Fig. 1A), possibly assisted by protractor hyoidei shortening (Fig. 1D).

As hypothesised previously for cichlid fishes (Aerts et al., 1987; Durie and Turingan, 2004), the contribution of the opercular mechanism to mouth opening in *C. gariepinus* is limited to the initial phase of mouth opening. The opercular mechanism generally has no effect on mouth opening during the second half of the mouth-opening phase in this catfish (Figs 6, 7). Given that lower jaw depression is resisted by forces resulting from the sub-ambient pressure inside the mouth cavity, and the inertia of the lower jaw is very low compared to these forces (Aerts et al., 1987; Van Wassenbergh et al., 2005), the inertia of the lower jaw will probably not result in any lower jaw rotation due to past force-input by the opercular mechanism.

The timing of rotation of the opercular bone with respect to mouth opening, however, is apparently not always identical when comparing different species. In our study species, the operculum stops its dorso-caudal rotation relatively early during the expansive phase of suction feeding. In other fishes, however, the maximal opercular rotation is reached near the moment of maximal mouth opening (Elshoud-Oldenhave and Osse, 1976; Lauder, 1982; Konow and Bellwood, 2005). Note, in this respect, that hyoid retraction and depression can interfere with opercular movement in some teleost species due to the presence of a ligament connecting the hyoid (epihyals or ceratohyals) to the interopercular bones (e.g. Anker, 1986). This ligament is typically present in Ctenosquamate fishes (i.e. Scopelomorpha and Acanthomorpha, which does not include catfishes; Stiassny, 1996) and may cause passive opercular rotation when the hyoid basis and interopercular are displaced dorso-caudally during the head expansion phase. In that case, observing opercular rotation does not necessary imply an active contribution of the opercular mechanism (Fig. 1A) to mouth opening. Yet, the angelfish *Pomacanthus semicirculatus,* for example, does not have this ligament connecting the hyoid to the interopercular and still performs opercular rotations approximately until the time of maximal gape (Konow and Bellwood, 2005). Consequently, the results presented here concerning duration of activity of the opercular mechanism in *C. gariepinus* may not reflect a pattern that is common to all teleost fishes.

Shortly after the start of mouth opening, the hyoid begins rotating ventrally and the protractor hyoidei coupling between the hyoid and the lower jaw becomes an important mouth-opener (mechanism 1C; Fig. 1C). Even without any protractor hyoidei shortening (mechanism 1D reinforcing the activity of mechanism 1C; Fig. 1D), this mechanism alone would be responsible for a large amount of mouth opening (approximately 70% of the total observed lower jaw rotation).

After the opercular mechanism (Fig. 1A) ceases to be active (on average after 45% of the mouth opening time), further mouth opening in *C. gariepinus* is exclusively achieved through the protractor hyoidei muscles (m-pr-h). This is done in a combination of four-bar mechanism 1C (Fig. 1C; ventral rotation of the m-pr-h origin by means of hyoid depression) and m-pr-h shortening (Fig. 1D). Mechanism 1C continues its contribution until maximal mouth opening, and is actively reinforced by m-pr-h shortening during this time. The m-pr-h now generally shortens 5–10% of its mean length (Figs 6, 7), which causes an extra 10–15° of lower jaw rotation in addition to the contribution of mechanism 1C (see above).

Mechanical basis of the two mouth-opening types

Two types of kinematic mouth-opening profiles were discerned in *C. gariepinus*: profiles that only have a single acceleration–deceleration and, the most commonly (67% of all cases), in which an additional deceleration–acceleration could be discerned (see Fig. 5). Surprisingly, such unusual characteristics of the mouth-opening kinematics have not yet been observed in other fishes, despite the large amount of

studies measuring mouth-opening kinematics (for a review, see Ferry-Graham and Lauder, 2001). Two options are possible: (1) mouth opening in the African catfish *C. gariepinus* is mechanically distinct from all previously studied fish; (2) the present marker-based, high-speed cineradiographic analysis generates kinematic profiles of higher resolution than most studies based on more common high-speed videography, and therefore allows discernment of more subtle variations in kinematics. This second option is not unlikely, since no such unexpected mouth-opening patterns were noticed during a preceding kinematic analysis of prey capturing *C. gariepinus*, in which images were obtained using a regular high-speed video camera, and manual, point-by-point digitisation of anatomic landmarks was done without the help of markers (Van Wassenbergh et al., 2004).

The present analysis of the mouth-opening mechanism may explain the mechanical causes of such distinct mouth-opening types. For one individual of this study (referred to as catfish A), mouth openings of each type are clearly driven by distinct mouth-opening mechanics. If there is no additional deceleration–acceleration, than maximal mouth opening is reached without any shortening of the protractor hyoidei muscles (Fig. 7A). In the other case (‘type 1’ mouth opening; Fig. 5), the protractor hyoidei do shorten, and the decelerating lower jaw is speeded up almost precisely at the time this muscle shortening starts (Fig. 6A). In addition, this individual can apparently modulate its maximal gape by opening the mouth with or without protractor hyoidei shortening during the second half of mouth opening (Fig. 5). This is in accordance with our observation that *C. gariepinus* is able to modulate maximum gape without changing the magnitude of hyoid depression when given prey of different sizes: as the opercular mechanism (Fig. 1A) only initiates mouth opening and mechanisms 1B and 1C (Fig. 1B,C) directly depend on the (equal) amount of hyoid depression, only protractor hyoidei shortening can achieve this.

However, in the two other individuals (referred to as catfishes B and C), mouth openings of both types were more similar in magnitude. The kinematic profiles from the different types could not be distinguished statistically and, in general, protractor hyoidei shortening also occurred in mouth openings without the additional acceleration–deceleration (Fig. 7B,C). Yet, in most cases, the start of the characteristic additional acceleration coincides with the start of protractor hyoidei shortening (Fig. 6B,C). As a result, although no distinctive mechanical basis for both mouth-opening types was found for these individuals, it is still likely that the observed phenomenon is related to the timing and/or speed of protractor hyoidei shortening.

Function of the angulo–ceratohyal ligament

The angulo–ceratohyal ligament (l-an-ch) connects the hyoid to the lower jaw (Fig. 1B). Previous functional morphological analyses have proposed that this ligament plays a part in mouth opening (see also Fig. 1B): the l-an-ch pulls the retro-articular process of the lower jaw backward during hyoid depression, which causes the lower jaw to depress (Diogo and Chardon, 2000; Adriaens et al., 2001). However, the results of the present study show that this ligament (being part of four-bar mechanism 1B; Fig. 1B) probably does not contribute at all to mouth opening in *C. gariepinus* (Figs 6, 7). The observed underprediction of the lower jaw angle (Figs 6, 7) during mouth opening in our analysis corresponds to a situation in which the length of the l-an-ch (four-bar coupler link) is shorter than prior to mouth opening (Fig. 9A). Unless the short l-an-ch is extremely elastic, this means that very little force will be transmitted to the lower jaw’s retro-articular process during mouth opening. Note that in the case where l-an-ch was indeed considerably elastic, the jaw adductors would probably need to be activated continuously when *C. gariepinus* is resting with its mouth closed. This is very unlikely, also given the fact that fully anaesthetised catfish do not show any signs of mouth opening. Manipulating the ligaments during dissections also proves it to be very poorly elastic.

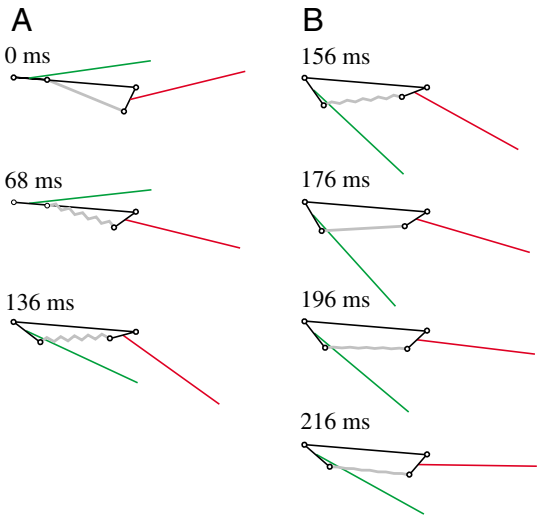

Fig. 9. A representative prey capture sequence of *C. gariepinus* showing a reconstruction of four-bar kinematics of mechanism 1B (Fig. 1B) during mouth opening (A) and mouth closing (B). Both the observed hyoid angle (green line) and lower jaw angle (red line) were used as input, whereas the length of the coupler link (i.e. the angulo–ceratohyal ligament; thick grey line) was adjusted to fit the observed hyoid and lower jaw kinematics. Note that the angulo–ceratohyal ligament elongates during mouth opening, but is stretched again during mouth closure, during which it helps to elevate the hyoid.

During mouth closing, however, our results indicate that the l-an-ch first increases in length to a point where it reaches its initial (i.e. prior to mouth opening) length (Fig. 9B). Next, hyoid and lower jaw kinematics are tightly coupled by the four-bar mechanism, in which the l-an-ch functions as a coupler link (Figs 6, 7). In contrast to mouth opening, the input force of the action by this four-bar system (Fig. 1B) no longer originates from the hyoid, but from the lower jaw (activity of the jaw adductor musculature during jaw closing). If we reverse the four-bar system described in Fig. 1B (crank becomes follower

and *vice versa*) then the results of Figs 6 and 7 can be interpreted as follows: hyoid elevation kinematics is accurately predicted by four-bar system 1B (Fig. 1B) with the measured, instantaneous lower jaw positions as input. In other words, the results of the present paper show that the l-an-ch functions as a hyoid-elevator: the l-an-ch linkage with the lower jaw is generally able to cause approximately 15–20° of hyoid elevation in *C. gariepinus*.

A ligament coupling lower jaw adduction to hyoid elevation can be important for a suction feeding fish's prey capture success. If a prey capture attempt is unsuccessful, then the hyoid will be automatically elevated. This will help in preparing a following attempt, because it is crucial to start a suction feeding act with a compressed buccal cavity (De Visser and Barel, 1996). These results also shed a different light on the function of the jaw adductors, which apparently not only power mouth closing, but indirectly also have an important role in hyoid elevation in the catfish studied. Note also that the protractor hyoidei coupling (Fig. 1C) may cooperate in hyoid elevation (see Figs 6, 7).

Hyoid-depression mechanisms

Hyoid depression in *C. gariepinus* is exclusively the result of mechanism 2A, involving neurocranial elevation and pectoral girdle retraction, caused by contraction of the epaxial and hypaxial musculature (Fig. 2A; Fig. 8). In this mechanism, the sternohyoideus muscle (m-sh) transmits the movement of the cleithral bone (part of the pectoral girdle) to the hyoid (Muller, 1987). Surprisingly, the m-sh does not shorten during hyoid depression and will therefore not reinforce the action of four-bar mechanism 2A (Fig. 2). In general, the m-sh even tends to elongate during hyoid depression (Fig. 8). Given the gradual nature of the measured m-sh elongation, this muscle clearly transmits the force from cleithral retraction during an eccentric contraction.

Even without the expected reinforcement by m-sh shortening, mechanism 2A (Fig. 2A) still causes the hyoid to depress extensively: the total hyoid rotation often exceeds 60°. Given the final hyoid configuration after rotations of this magnitude, any further depression of the hyoid by m-sh shortening would probably cause a considerable caudal displacement of the hyoid tip, but relatively little lowering of the mouth floor and thus little extra volume increase of the buccal cavity (causing additional water inflow). This may explain why m-sh shortening, or even keeping the m-sh at the same length, is not needed for this species to perform successful prey captures.

On the other hand, m-sh shortening during hyoid depression would theoretically increase the speed of hyoid depression, and indirectly also the speed of mouth opening (through the mechanism shown in Fig. 1C). In fact, our results indicate some limited m-sh shortening during the prey captures in which the fastest hyoid depressions are generated: if the kinematic data from the five sequences with the fastest hyoid depressions are pooled, then two of the three individuals (A and B) show, respectively, 3% and 4% m-sh shortening between 52–85% and 20–54% of the mouth opening phase. However, even in these sequences, the final m-sh length at maximal hyoid depression is considerably larger than its length at the start of hyoid expansion. Furthermore, in one individual (C) the m-sh elongation pattern during the fastest hyoid depressions did not differ from all other sequences (Fig. 8C).

Therefore, we hypothesise that the m-sh in *Clarias gariepinus* is not powerful enough to perform a constant, concentric contraction when it is being retracted by the cleithrum. This depression of the cleithrum is powered by the hypaxial and epaxial muscles, which together have a much larger mass than the m-sh (Herrel et al., 2005). Consequently, a lot of force will be needed to resist elongation when the powerful hypaxials and epaxials contract, so that the m-sh can probably not contract during this time. Note, however, that other clariid species (e.g. *Clariallabes longicauda*) have a much larger cross-sectional area of the m-sh compared to *Clarias gariepinus* (Van Wassenbergh et al., 2004). Therefore, it is not impossible that this morphological difference will be reflected by a different pattern of m-sh length changes during hyoid depression, especially given the fact that maximal hyoid depressions are also larger in these species (Van Wassenbergh et al., 2004).

Note also that shortening of the sternohyoideus during hyoid depression has been observed in the sunfish *Micropterus salmoides* (Carroll, 2004). Consequently, the hyoid depression mechanics discussed in this study for *Clarias gariepinus* certainly do not apply to all teleost fishes. Logically, the same is also true for the mechanics of the sternohyoideus observed in the above-mentioned sunfish from the study by Carroll (2004).

Thanks to Jeannine Fret for assistance during implanting of the markers and during the many unsuccessful EMG experiments. We also thank Bieke Vanhooydonck and the two anonymous reviewers for help in revising the manuscript. The authors gratefully acknowledge support of the Special Research Fund of the University of Antwerp to S.V.W. The research was further supported by the FWO grant G.0355.04. A.H. is a postdoctoral fellow of the Fund for Scientific Research – Flanders (FWO-Vl).

References

Adriaens, D., Aerts, P. and Verraes, W. (2001). Ontogenetic shift in mouth opening mechanisms in a catfish (Clariidae, Siluriformes): a response to increasing functional demands. *J. Morphol.* **247**, 197-216.

Aerts, P. (1991). Hyoid morphology and movements relative to abducting forces during feeding in *Astatotilapia elegans* (Teleostei: Cichlidae). *J. Morphol.* **208**, 323-345.

Aerts, P. and Verraes, W. (1984). Theoretical analysis of a planar four bar system in the teleostean skull: the use of mathematics in biomechanics. *Ann. Soc. R. Zool. Belg.* **114**, 273-290.

Aerts, P., Osse, J. W. M. and Verraes, W. (1987). Model of jaw depression during feeding in *Astatotilapia elegans* (Teleostei: Cichlidae). Mechanisms for energy storage and triggering. *J. Morphol.* **194**, 85-109.

Alexander, R. M. (1965). Structure and function in catfish. *J. Zool. (London)* **148**, 88-152.

Alexander, R. M. (1970). Feeding. In *Functional Design in Fishes*, pp. 89-114. London: Hutchinson University Press.

Anker, G. C. (1986). The morphology of joints and ligaments in the head of a generalized *Haplochromis* species: *H. elegans trewavas* 1933 (Teleostei, Cichlidae). I. The infraorbital apparatus and the suspensorial apparatus. *Neth. J. Zool.* **36**, 498-530.

Bergert, B. A. and Wainwright, P. C. (1997). Morphology and kinematics of prey capture in the syngnathid fishes *Hippocampus erectus* and *Syngnathus floridae*. *Mar. Biol.* **127**, 563-570.

Carroll, A. M. (2004). Muscle activation and strain during suction feeding in the largemouth bass *Micropterus salmoides. J. Exp. Biol*. **207**, 983-991.

De La Hoz, E. U. (1994). Aspectos cinemáticos del mecanismo de mordida premaxilar en los géneros Cauque, Basilichthys y Austromenidia (Teleostei, Atherinidae). *Invest. Mar.* **22**, 31-37.

De La Hoz, E. U., Cancino, C. A. and Ojeda, E. J. (1994). De capacidades de modulación y plasticidad funcional de los mecanismos de captura de alimento en *Atherinopsinae sudamericanos* (Teleostei, Atherinidae). *Invest. Mar.* **22**, 45-65.

De Visser, J. and Barel, C. D. N. (1996). Architectonic constraints on the hyoid's optimal starting position for suction feeding of fish. *J. Morphol.* **228**, 1-18.

Diogo, R. and Chardon, M. (2000). Anatomie et fonction des structures céphaliques associées à la prise de nourriture chez le genre *Chrysichthys* (Téléostei: Siluriformes). *Belg. J. Zool.* **130**, 21-37.

Durie, C. J. and Turingan, R. G. (2004). The effects of opercular linkage disruption on prey-capture kinematics in the teleost fish *Sarotherodon melanotheron*. *J. Exp. Zool.* **301**, 642-653.

Elshoud-Oldenhave, M. J. W. and Osse, J. W. M. (1976). Functional morphology of the feeding system in the ruff *Gymnocephalus cernua* (L. 1758) – (Teleostei, Percidae). *J. Morphol.* **150**, 399-422.

Ferry-Graham, L. A. and Lauder, G. V. (2001). Aquatic prey capture in ray-finned fishes: a century of progress and new directions. *J. Morphol.* **248**, 99-119.

Ferry-Graham, L. A., Wainwright, P. C., Hulsey, C. D. and Bellwood, D. R. (2001). Evolution and mechanics of long jaws in butterflyfishes (Family Chaetodontidae). *J. Morphol.* **248**, 120-143.

Gibb, A. C. (2003). Modeling the jaw mechanism of *Pleuronichthys verticalis*: the morphological basis of assymetrical jaw movement in a flatfish. *J. Morphol.* **265**, 1-12.

Herrel, A., Van Wassenbergh, S., Wouters, S., Adriaens, D. and Aerts, P. (2005). A functional morphological approach to the scaling of the feeding system in the African catfish, *Clarias gariepinus*. *J. Exp. Biol.* **208**, 2091-2102.

Hulsey, C. D. and Wainwright, P. C. (2002). Projecting mechanics into morphospace: disparity in the feeding system of labrid fishes. *Proc. R. Soc. Lond. B* **269**, 317-326.

Konow, N. and Bellwood, D. (2005). Prey-capture in *Pomacanthus semicirculatus* (Teleostei, Pomacanthidae): functional implications of intramandibular joints in marine angelfishes. *J. Exp. Biol.* **208**, 1421-1433.

Lauder, G. V. (1982). Patterns of evolution in the feeding mechanism of Actinopterygian fishes. *Am. Zool.* **22**, 275-285.

Motta, P. J. (1984). Mechanics and function of jaw protrusion in fishes: a review. *Copeia* **1984**, 1-18.

Muller, M. (1987). Optimization principles applied to the mechanism of neurocranium levation and mouth bottom depression in bony fishes (Halecostomi). *J. Theor. Biol.* **126**, 343-368.

Muller, M. (1996). A novel classification of planar four-bar linkages and its application to the mechanical analysis of animal systems. *Phil. Trans. R. Soc. Lond. B* **351**, 689-720.

Otten, E. (1982). The development of a mouth-opening mechanism in a generalized *Haplochromis* species: *H. elegans* Trewavas 1933 (Pisces, Cichlidae). *Neth. J. Zool*. **32**, 31-48.

Stiassny, M. L. J. (1996). Basal ctenosquamate relationships and the interrelationships of the myctophiform (scopelomorph) fishes. In *Interrelationships of Fishes* (ed. M. L. J. Stiassny, L. R. Parenti and G. D. Johnson), pp. 405-426. London: Academic Press.

Teugels, G. G. (1996). Taxonomy, phylogeny and biogeography of catfishes (Ostariophysi, Siluroidei): An overview. *Aquat. Liv. Res.* **9**, 9-34.

Van den Berg, C. (1994). A quantitative, three-dimensional method for analyzing rotational movement from single-view movies. *J. Exp. Biol.* **191**, 283-290.

Van Dobben, W. H. (1937). Über den Kniefermechanismus der Knochenfishe. *Arch. Néerl. D Zool.* **3**, 1-72.

Van Wassenbergh, S., Herrel, A., Adriaens, D. and Aerts, P. (2004). Effects of jaw adductor hypertrophy on buccal expansions during feeding of air breathing catfishes (Teleostei,Clariidae). *Zoomorphol.* **123**, 81-93.

Van Wassenbergh, S., Aerts, P. and Herrel, A. (2005) Scaling of suction-feeding kinematics and dynamics in the African catfish, *Clarias gariepinus*. *J. Exp. Biol.* **208**, 2103-2114.

Wainwright, P. C., Alfaro, M. E., Bolnick, I. and Hulsey, D. (2005). Many-to-one mapping of form to function: a general principle in organismal design? *Integr. Comp. Biol.* **45**, 256-262.

Waltzek, T. B. and Wainwright, P. C. (2003). Functional morphology of extreme jaw protrusion in neotropical cichlids. *J. Morphol*. **257**, 96-106.

Westneat, M. W. (1990). Feeding mechanics of teleost fishes (Labridae; Perciformes): a test of four-bar linkage models. *J. Morphol.* **205**, 269-295.

Westneat, M. W. (1994). Transmission of force and velocity in the feeding mechanism of labrid fishes (Teleostei, Perciformes). *Zoomorphol.* **114**, 103-118.

Westneat, M. W. (2004). Evolution of levers and linkages in the feeding mechanisms of fishes. *Integr. Comp. Biol.* **44**, 378-389.

Westneat, M. W. and Wainwright, P. C. (1989). Feeding mechanisms of *Epibulus insidiator* (Labridae; Teleostei): evolution of a novel functional system. *J. Morphol.* **202**, 129-150.

Winter, D. A. (2004). *Biomechanics and Motor Control of Human Movement*. 3rd edn. Hoboken, NJ, USA: John Wiley and Sons.